The Synergistic Interactions of Allergic Lung Inflammation and Intratracheal Cationic Protein

On-line Data Supplement

Jason H.T. Bates, Ana Cojocaru, Hans C. Haverkamp, Lisa M. Rinaldi, and Charles G. Irvin

Vermont Lung Center, Departments of Medicine and Molecular Physiology and Biophysics, University of Vermont, Burlington, VT 05405-0075

METHODOLOGIC DETAILS

Preparation of Animal Models

Naïve groups: Mice were anesthetized with pentobarbital sodium by intraperitoneal injection (90 ml/kg diluted in phosphate-buffered saline to 5 mg/ml), tracheostomized, and an 18-gauge cannula tied into the trachea for mechanical ventilation.

Ova groups: Mice were sensitized with an intra-peritoneal injection of ovalbumin (20 μg in 2.25 mg alum) on days 0 and 14. They were challenged on each of days 21, 22 and 23 by being placed in a compartmentalized aerosolization chamber and exposed to ovalbumin aerosol (1% in phosphate-buffered saline) for 30 min. On day 25, the mice were anesthetized, tracheostomized and cannulated as above.

PLL groups: Mice were anesthetized and tracheostomized as above. A length of polyethylene tubing was passed into the trachea to allow instillation of 33 μg of PLL in 50 μl of a phosphate-buffered solution, followed by three 0.3 ml aliquots of air in order to flush the PLL into the lung, as previously described (1, 2). Next, an 18-gauge metal cannula was secured in the tracheal opening ready for mechanical ventilation, and ¼ of the original dose of sodium pentobarbital was given.

PLL+Ova groups: The procedures for the Ova and PLL groups described above were combined.

The group numbers were as follows. For the BALB/c strain, Naïve n = 8, PLL n = 7, Ova n = 7, PLL+Ova n = 6. For the A/J strain, Naïve n = 8, PLL n = 8, Ova n = 9, PLL+Ova n = 7. For the C57BL/6 strain, Naïve n = 8, PLL n = 8, Ova n = 5, PLL+Ova n = 6.

Measurement of Respiratory Mechanical Impedance

The pressure and flow data obtained during application of each volume perturbation were used to calculate a complex input impedance of the respiratory system (Z_{rs}) after digital removal of the mechanical effects of the ventilator circuit, as previously described (3). Z_{rs} was fit to the equation of a lung model consisting of a single airway serving a constant-phase viscoelastic tissue unit. The model equation is (4)

$$Z(f) = R + i2\pi fI + \frac{G - iH}{(2\pi f)^{\alpha}} \qquad \text{(S-1)}$$

where R is a Newtonian resistance composed mostly of the flow-resistance of the conducting pulmonary airways (5), I reflects the inertance of the gas in the central airways, G reflects viscous dissipation of energy in the respiratory tissues (tissue resistance), H reflects elastic

energy storage in the tissues (tissue stiffness), *f* is frequency, $i = \sqrt{-1}$, and α couples *G* and *H* (4).

This model has been shown to accurately describe respiratory impedance between 0 and 20 Hz under control conditions and during bronchoconstriction (3, 4, 6). We thus obtained a time-course of the parameters *R*, *I*, *G* and *H* for the 5 min following bronchial challenge in the mice. *I* has negligible effect in the mouse lung below 20 Hz, and so can be ignored (3). Therefore, we confine our attention to the parameters *R*, *G* and *H*.

Computational model of the mouse lung

We constructed a computational model of the mechanics of the mouse lung, as in our recent previous studies (7-9) following the asymmetrical branching scheme of Horsfield (10). The airway structural data were taken from Gomes and Bates (11), with their airway radii being divided by the factor 1.1 in order to make the simulated baseline values of *R* match the experimental baseline values. Random values were assigned to the baseline (unconstricted) radii of the airways in the model according to Gaussian distributions having means and standard deviations appropriate to the airway order as per the data tabulated for the mouse lung by Gomes and Bates (11). The impedance of each airway (Z_{aw}) in the model was calculated, assuming Poiseuille flow, to determine resistance and the mass of the airway gas to determine inertance as follows:

$$Z_{aw}(f) = \frac{8\mu L}{\pi r^4} + i\frac{2fL\rho}{r^2} \qquad \text{(S-2)}$$

where r is airway radius, L is airway length, μ is gas viscosity, and ρ is gas density. Each of the most distal airways terminated in an identical tissue unit with impedance given, in analogy with Eq. S-1 of the manuscript, by

$$Z_{ti}(f) = \frac{G_{ti} - H_{ti}}{(2\pi f)^{\alpha}} \tag{S-3}$$

with H_{ti} having a value of 2000 $cmH_2O.s.ml^{-1}$ and the baseline ratio G_{ti}/H_{ti} being assigned a value of 0.042 (7). We found, by trial and error that, in order to achieve a good match between the simulated and experimental G profiles, it was necessary to increase the G_{ti}/H_{ti} during bronchoconstriction according to the formula

$$\frac{G_{ti}}{H_{ti}} = 0.1\left(1 + 3F_{closed}\right) \tag{S-4}$$

where F_{closed} is the fraction of the lung volume behind closed airways at any given point in time. Equation S-4 accounts empirically for the increase in G_{ti}/H_{ti} that has been observed experimentally during bronchoconstriction in animals (12) and in isolated tissue strips (13).

F_{closed} was determined at each point during the simulation by the number of tissue units located behind closed airways. Airway closure was produced in the model by closing any airway whose radius narrowed to a predetermined critical value. We assume here that airway closure (i.e. derecruitment of lung units) is due to the formation of liquid bridges across the airway lumen and accounts for the post-methacholine plateaus in H that are always observed experimentally (7, 8). This assumption is based on the supposition of negligible homogenizing effect of collateral ventilation (14), and is supported by the fact that these plateaus in H are reversed by a deep lung

inflation. We also recently used micro-computed tomography to show that the elevations in *H* correspond to the amount of derecruited lung in allergically inflamed mice (15).

The total impedance of the model, Z_{mod}, was calculated by adding the individual Z_{aw} and Z_{ti} in series or parallel, as appropriate. Z_{mod} was calculated at each of the frequencies in the volume perturbation signal used to obtain Z_{rs} experimentally. The Monte-Carlo approach was used to obtain mean ± SE for Z_{mod} by running the computational model 8 times for each condition, each time using a different statistical realization of the airway radii values. To determine the transient fractional decrease in airway diameters needed to create a simulated time-course for *R* matching that observed experimentally, the mean experimental profile of *R* was normalized to its initial value, inverted, and the fourth root of the result taken. We found by trial and error that the fractional changes from 1 in the resulting profile had to be scaled by the factor 1.3 to achieve a good match between simulated and experimental *R* profiles for the Naïve and PLL groups. The factor was reduced to 1.0 for the Ova and PLL+Ova groups, reflecting the reduced degree of smooth muscle shortening caused by the increased barrier function of the inflamed mucosa in these two groups.

To simulate the combined effects of cationic protein and antigen treatment, we combined the features present in our previous model simulations; 1) an 18 micron thick lining was added to all airways in the model (to represent epithelial thickening), 2) the critical threshold radius at which airways close was increased from 38 microns to 45 microns (to simulate the effect of increased airway secretions), and 3) the airways of the model were forced to follow a fractional narrowing profile matching that of the PLL group (to represent enhanced smooth muscle shortening).

Single airway model of synergy

Consider a cylindrical airway with internal radius r_0 in the baseline unconstricted state (Fig. E-1). If the smooth muscle surrounding the airway wall shortens circumferentially by a fraction α of its baseline length, airway radius will decrease by the same fraction, where $0 < \alpha < 1$. Assuming Poiseuille flow through the airway, this will cause R_{aw} to increase by the factor $1/(1 - \alpha)^4$. Alternatively, the same increase in R_{aw} will occur if the airway wall thickens inward to occupy the fraction α of the original lumen radius, in which case the area (A) of the airway wall is

$$\begin{aligned} A &= \pi r_0^{\,2} - \pi\left[r_0(1-\alpha)\right]^2 \\ &= \pi r_0^{\,2}\alpha(2-\alpha) \end{aligned} \qquad \text{(S-5)}$$

Now suppose that the smooth muscle shortens by the fraction α when the airway walls are already thickened as in Eq. S-5, producing a lumen radius r_l. If we assume that A remains fixed as the airway narrows, then

$$A = \pi\left[r_0(1-\alpha)\right]^2 - \pi r_l^{\,2} \qquad \text{(S-6)}$$

Combining Eqs. S-5 and S-6 and rearranging gives

$$r_l = r_0\sqrt{1-4\alpha+2\alpha^2} \qquad \text{(S-7)}$$

This corresponds to an increase in R_{aw} by the factor $1/\left(1-4\alpha+2\alpha^2\right)^2$, which reaches infinity when $\alpha = 1-1/\sqrt{2} \approx 0.3$.

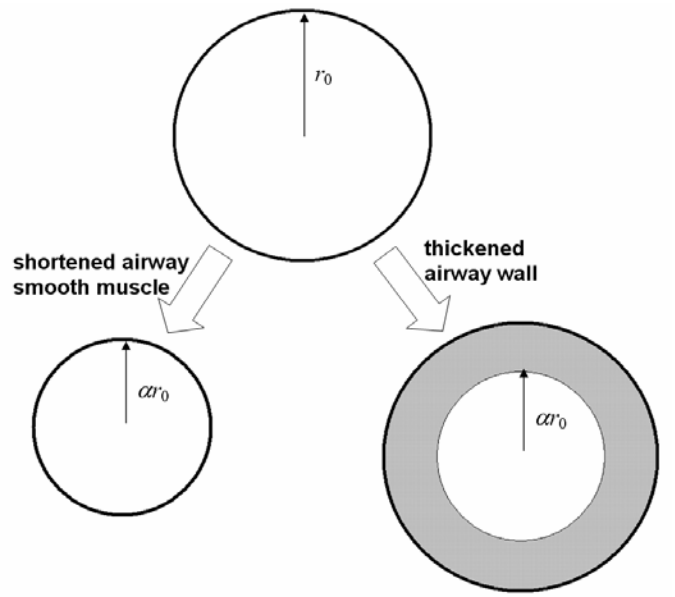

Figure E-1: Simple model of a single constricting airway with baseline radius r_0. We consider narrowing of this airway by two distinct mechanisms: 1) shortening of the airway smooth muscle by a factor $\alpha < 1$, and 2) thickening of the bronchial mucosa such that the airway lumen is reduced by the same factor.

ADDITIONAL RESULTS

Figure E-2 shows dose-response relationships for airway resistance (*R*) and tissue stiffness (*H*) obtained from measurements of input impedance following sequential challenges with increasing doses of methacholine aerosol in four groups of A/J mice (left-hand panels) and C57BL/6 mice (right-hand panels): The four experimental groups in each mouse strain are 1) untreated (Naïve), 2) treated with intra-tracheal cationic protein (PLL), 3) antigen sensitized and challenged (Ova), and 4) treated with both cationic protein and antigen (PLL+Ova). The A/J mice behaved in a qualitatively similar fashion to the BALB/c mice (see Fig. 1 of manuscript); ova treatment alone caused *H* to become elevated compared to the naïve animals, while the combination of ova plus PLL caused a substantial elevation in the greater degree of hyprresponsiveness in *H* (especially at intermediate doses of methacholine). By contrast, ova treatment in the C57BL/6 mice did not cause either *H* or *R* to become elevated compared the naïve group, and there was no synergistic

effect due to ova and PLL treatments together. PLL treatment cause hyperresponsiveness in both strains.

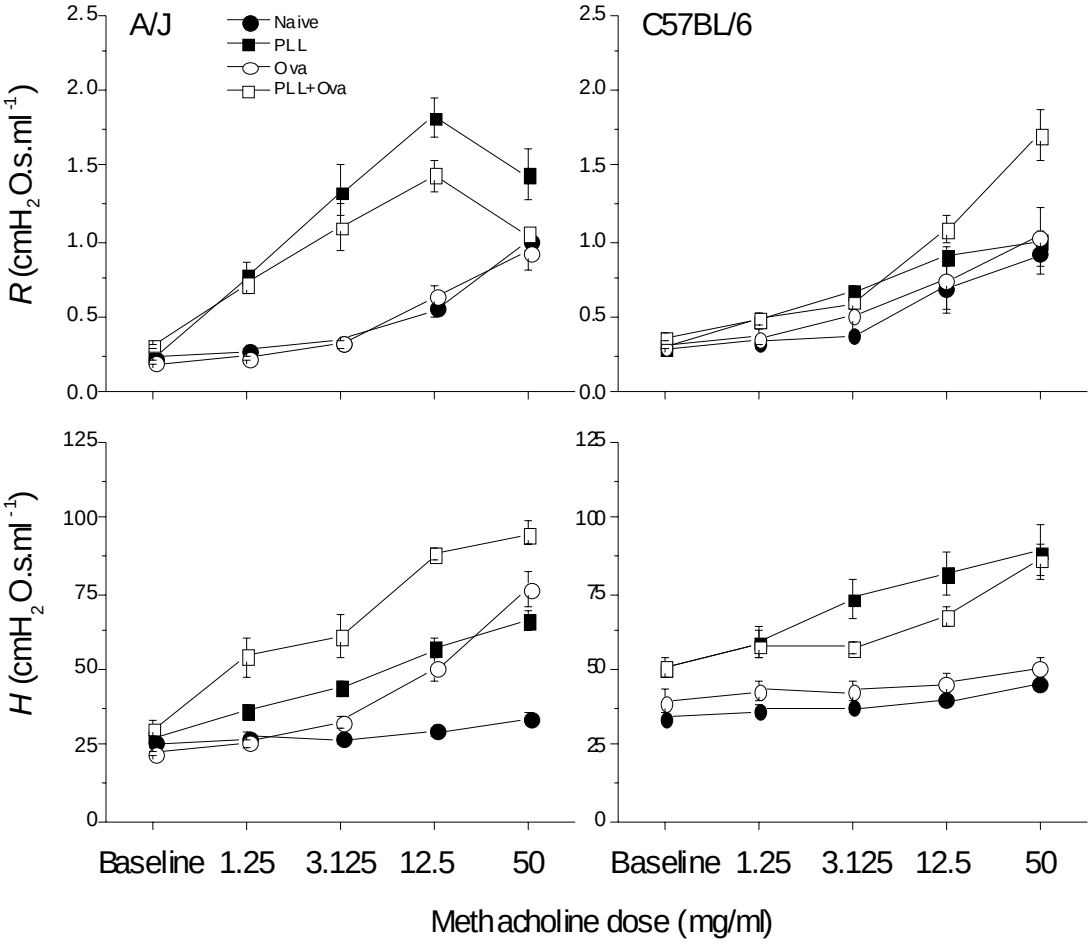

Figure E-2: Dose-response curves for the impedance parameters *R* and *H* for the A/J and C57BL/6 strains of mice.

REFERENCES

E1. Coyle, A. J., S. J. Ackerman, and C. G. Irvin. 1993. Cationic proteins induce airway hyperresponsiveness dependent on charge interactions. *Am Rev Respir Dis* 147(4):896-900.

E2. Homma, T., J. H. Bates, and C. G. Irvin. 2005. Airways Hyperresponsiveness Induced by Cationic Proteins In Vivo: Site of Action. *Am J Physiol Lung Cell Mol Physiol* 289:L413-L418.

E3. Gomes, R. F., X. Shen, R. Ramchandani, R. S. Tepper, and J. H. Bates. 2000. Comparative respiratory system mechanics in rodents. *J Appl Physiol* 89(3):908-16.

E4. Hantos, Z., B. Daroczy, B. Suki, S. Nagy, and J. J. Fredberg. 1992. Input impedance and peripheral inhomogeneity of dog lungs. *J Appl Physiol* 72(1):168-78.

E5. Tomioka, S., J. H. Bates, and C. G. Irvin. 2002. Airway and tissue mechanics in a murine model of asthma: alveolar capsule vs. forced oscillations. *J Appl Physiol* 93(1):263-70.

E6. Petak, F., Z. Hantos, A. Adamicza, T. Asztalos, and P. D. Sly. 1997. Methacholine-induced bronchoconstriction in rats: effects of intravenous vs. aerosol delivery. *J Appl Physiol* 82(5):1479-87.

E7. Bates, J. H. T., S. S. Wagers, R. J. Norton, L. M. Rinaldi, and C. G. Irvin. 2006. Exaggerated Airway Narrowing in Mice Treated with Intra-Tracheal Cationic Protein. *J Appl Physiol* 100:500-506.

E8. Wagers, S., L. K. Lundblad, M. Ekman, C. G. Irvin, and J. H. T. Bates. 2004. The allergic mouse model of asthma: normal smooth muscle in an abnormal lung? *J Appl Physiol* 96(6):2019-27.

E9. Wagers, S. S., H. C. Haverkamp, J. H. T. Bates, R. J. Norton, J. A. Thompson-Figueroa, M. J. Sullivan, and C. G. Irvin. 2007. Intrinsic and antigen-induced airway hyperresponsiveness are the result of diverse physiological mechanisms. *J Appl Physiol* 102(1):221-30.

E10. Horsfield, K., W. Kemp, and S. Phillips. 1982. An asymmetrical model of the airways of the dog lung. *J Appl Physiol* 52(1):21-6.

E11. Gomes, R. F., and J. H. Bates. 2002. Geometric determinants of airway resistance in two isomorphic rodent species. *Respir Physiolo Neurobiol* 130(3):317-25.

E12. Bates, J. H. T., A. M. Lauzon, G. S. Dechman, G. N. Maksym, and T. F. Schuessler. 1994. Temporal dynamics of pulmonary response to intravenous histamine in dogs: effects of dose and lung volume. *J Appl Physiol* 76(2):616-26.

E13. Fredberg, J. J., D. Bunk, E. Ingenito, and S. A. Shore. 1993. Tissue resistance and the contractile state of lung parenchyma. *J Appl Physiol* 74(3):1387-97.

E14. Brown, R., A. J. Woolcock, N. J. Vincent, and P. T. Macklem. 1969. Physiological effects of experimental airway obstruction with beads. *J Appl Physiol* 27(3):328-35.

E15. Lundblad, L. K., J. Thompson-Figueroa, G. B. Allen, L. Rinaldi, R. J. Norton, C. G. Irvin, and J. H. T. Bates. 2007. Airways Hyperresponsiveness in Allergically Inflamed Mice: The Role of Airway Closure. *Am J Respir Crit Care Med* 175:768-774.